Electrical Power and Energy Systems 160 (2024) 110086

Contents lists available at ScienceDirect

International Journal of Electrical Power and Energy Systems

journal homepage: www.elsevier.com/locate/ijepes

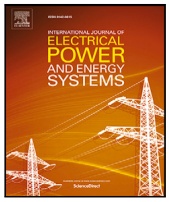

A novel wide-area control for general application to inverter-based resources in power systems

Mariano G. Ippolito, Rossano Musca *

Engineering Department, University of Palermo, V.le delle Scienze, Palermo, 90128, Italy

ARTICLE INFO

Keywords:
Damping
Grid-following
Grid-forming
Inverter-based resources
Latency
Wide-area damping control

ABSTRACT

The article illustrates the wide-synchronization control, a novel wide-area control for general application to inverter-based resources. The principle is first introduced from a theoretical point of view, including a mathematical proof of the concept, a technological assessment of grid-following and grid-forming converters as actuators, and the examination of the effects of the latencies. The wide-synchronization control is then demonstrated with the application to two case-studies, the standard two-area benchmark system and the large-scale European power system. Analysis and results indicate that the proposed control can remarkably improve the dynamic characteristics of the system, securing a stable operation with a high degree of flexibility and even under critical conditions.

1. Introduction

Modern power systems are evolving towards high integration of renewable energy sources, with massive penetration levels of power converters technologies, heavily stressed operating conditions, and increasing vulnerability against contingencies. In this rapid transformation, expansion and reinforcement of the system struggle to keep the same pace. Power systems are then experiencing considerable challenges, especially related to major stability issues. In this context, power system oscillations are an essential aspect which has to be addressed [1,2]. System oscillations are generated as a characteristic of interconnected power systems and power transfer operations, and must be contained since they can degrade the capabilities of the system. In worst cases of poorly damping conditions, these oscillations can even cause the instability of the system, leading to partial or total power outages [3]. The use of local controllers such as the power system stabilizers (PSSs) connected to synchronous machines is often not sufficient to damp the inter-area oscillations in the system. Wide-area damping control is an alternative and modern solution to effectively damp system oscillations, supported by recent advancements in the wide-area measurement system (WAMS) and increasing integration of phasor measurement units (PMUs) in the system [4,5]. The conventional actuators of wide-area control schemes are the PSSs, with the provision of supplementary damping control signals. Recently, with the development and the integration of power converters, other technological solutions have been considered as wide-area control actuators, such as flexible AC transmission system (FACTS) devices, high voltage direct current (HVDC) stations, renewable-based power plants and storage systems [6]. The three main types of actuators, i.e. PSSs, FACTS and HVDC, present both advantages and disadvantages [7–9]. PSSs and FACTS are widely used in power systems, and they also offer a high control efficiency. However, both PSSs and FACTS provide damping indirectly, by controlling voltage and reactive power. HVDC systems have the advantages of directly controlling the active power, with fast and flexible control actions, offering also a large adjustable capability. HVDC systems, however, are not distributed in the power system as PSSs controllers of synchronous machines and FACTS devices, and the damping performances might be affected by their locations. Several works in literature address different types of wide-area control actuators. For instance, application and design of a STATCOM-based wide-area damping control is discussed in [10]. Doubly fed induction generators of wind power plants are used as actuators in the wide-area control presented in [11]. The wide-area control proposed in [12] implements a coordination between the HVDC controller of doubly fed induction generators and FACTS devices. A wide-area damping controller based on thyristor controlled series compensators (TCSC) is presented in [13]. The wide-area control discussed in [14] considers wind power plants and superconducting magnetic energy storage with damping controllers. The application of a static VAR compensator (SVC) as actuator of a wide-area damping control is discussed in [15]. A wide-area control employing the energy storage systems represented by large-scale fleet of electric vehicles is proposed in [16].

Although various possibilities have been studied, a research gap exists in the definition of a common wide-area control for application to different technologies and different types of actuators. Also, the

* Corresponding author.
E-mail address: rossano.musca@unipa.it (R. Musca).

https://doi.org/10.1016/j.ijepes.2024.110086
Received 9 January 2024; Received in revised form 9 May 2024; Accepted 12 June 2024
Available online 1 July 2024

emerging technology of grid-forming control for power converters has not been considered for application in wide-area damping controls.

1.1. Novelty and contribution

Inverter-based resources can support the system for different aspects, such as frequency control and local damping provision. This work investigates the application of inverter-based resources to a novel wide-area control scheme, presenting a general and comprehensive formulation. The definition of the proposed concept is intended for general application to the inverter-based resources in the system. The concept is denominated wide-synchronization control (WSC), and it basically relies on a reference frequency signal as main feedback of the control. The reference frequency is provided as remote signal to the resources participating in the control, and it is ultimately used to determine a transient adjustment of the active power of the inverter-based resources. This wide-area control concept can be implemented both on grid-following and grid-forming control structures. For that, the article resumes the work of the authors in [17], presenting an alternative implementation of the WSC for general application to any inverter-based resource. In the previous works of the authors, the focus was the grid-forming technology, and the WSC was implemented as an internal modification of the synchronization control loop of the grid-forming converter. In this work, an alternative formulation of the WSC concept is presented, relying on an independent external control block rather than an internal modification of the control structure, thus leading to a general application of the WSC to any inverter-based resource. For that, an original theoretical formulation not present in existing literature is provided. In comparison with previous works, the novelty of this paper can be therefore summarized in the following points:

- generalization of the proposed concept, extending to any inverter-based resource;
- theoretical definition of the damping coupling concept, as the driving force of the proposed control;
- analytical investigation of the effect of the latencies, with particular focus on the root causes;
- comprehensive demonstration of the capabilities of the concept, also under critical conditions.

The proposed concept is particularly addressed to Transmission System Operators (TSO), but also inverter manufacturers and power plant owners can be related, as this control action might be a service specified by grid codes and possibly subject to a remuneration scheme.

1.2. Organization

The remaining part of the paper is organized as follows. Concept and main characteristics of the proposed control are presented in Section 2. A technological assessment about relying on grid-forming or grid-following power converters as wide-area actuators is provided, describing advantages and disadvantages of both solutions. The concept is then discussed from a theoretical point of view in Section 3, illustrating the mathematical background and providing a deep insight about the principles of the control. Section 4 addresses the impact of latencies and time delays on the WSC with a formal analysis, also providing a representative example. The theoretical considerations are demonstrated with two different case-studies in Section 5, considering the standard two-area benchmark system and the large-scale model of the European power system. In Section 6, open points and possible further research are finally discussed.

2. Wide-synchronization control

2.1. General concept

The concept of the WSC substantially consists in a transient change of the active power output of the inverter-based resources. The transient change in the active power is determined according to the difference between the local frequency measurement and a remote reference frequency, which should represent the average behaviour of the power system. The basic idea is resumed from the concept developed by the authors in previous works [17–19]. The principle of the WSC can be ultimately summarized by:

$$\Delta p^* = K_w \left(f_{\text{sys}} - f \right) \tag{1}$$

where Δp^* is the change in active power locally realized by the inverter-based resource, K_w is the control gain, f is the local frequency, and f_{sys} is the remote reference signal provided by a computation unit of the wide-area control. According to the principle of the WSC, the reference signal f_{sys} should correspond to the average frequency of the system, and it is generally given by:

$$f_{\text{sys}} = \frac{1}{N_m} \sum_{m=1}^{N_m} f_m \tag{2}$$

where N_m is the number of frequency measurements, sent to the computation unit of the wide-area control for the determination of the average value. Independently on the given control structure of the inverter-based resources, the reference setpoint of the active power can be then adjusted according to (1), for the actuation of the proposed control. The inverter-based resources participating in the WSC control can be either controlled with grid-following or grid-forming strategies. These two technologies are extensively studied and compared [20], also in terms of damping and power system oscillations [21–23]. Figs. 1 and 2 show the block diagrams of possible grid-following and grid-forming

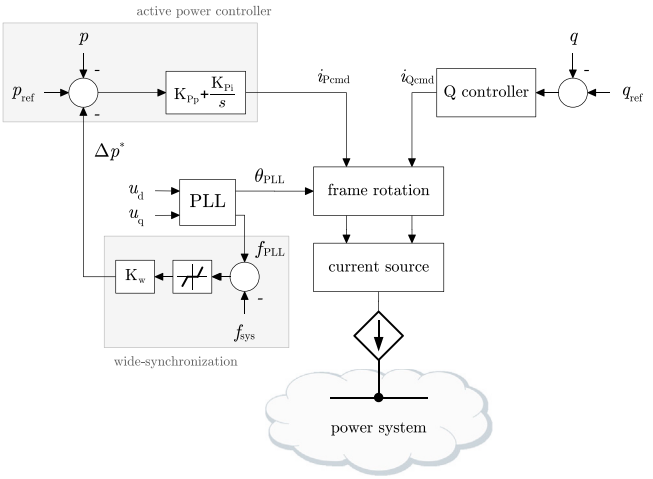

Fig. 1. Implementation of the WSC in a grid-following control structure.

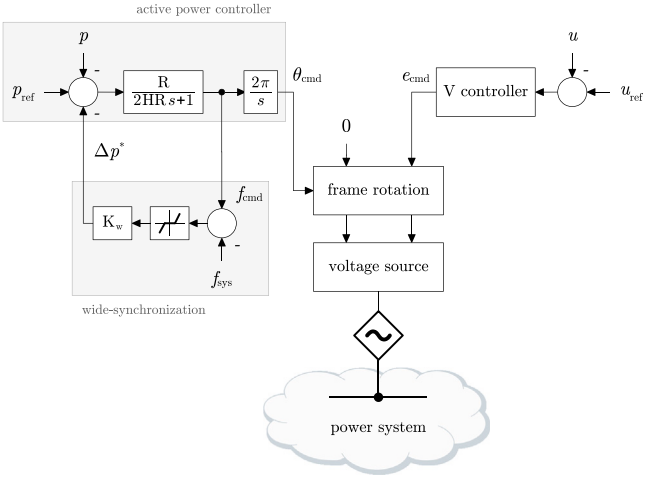

Fig. 2. Implementation of the WSC in a grid-forming control structure.

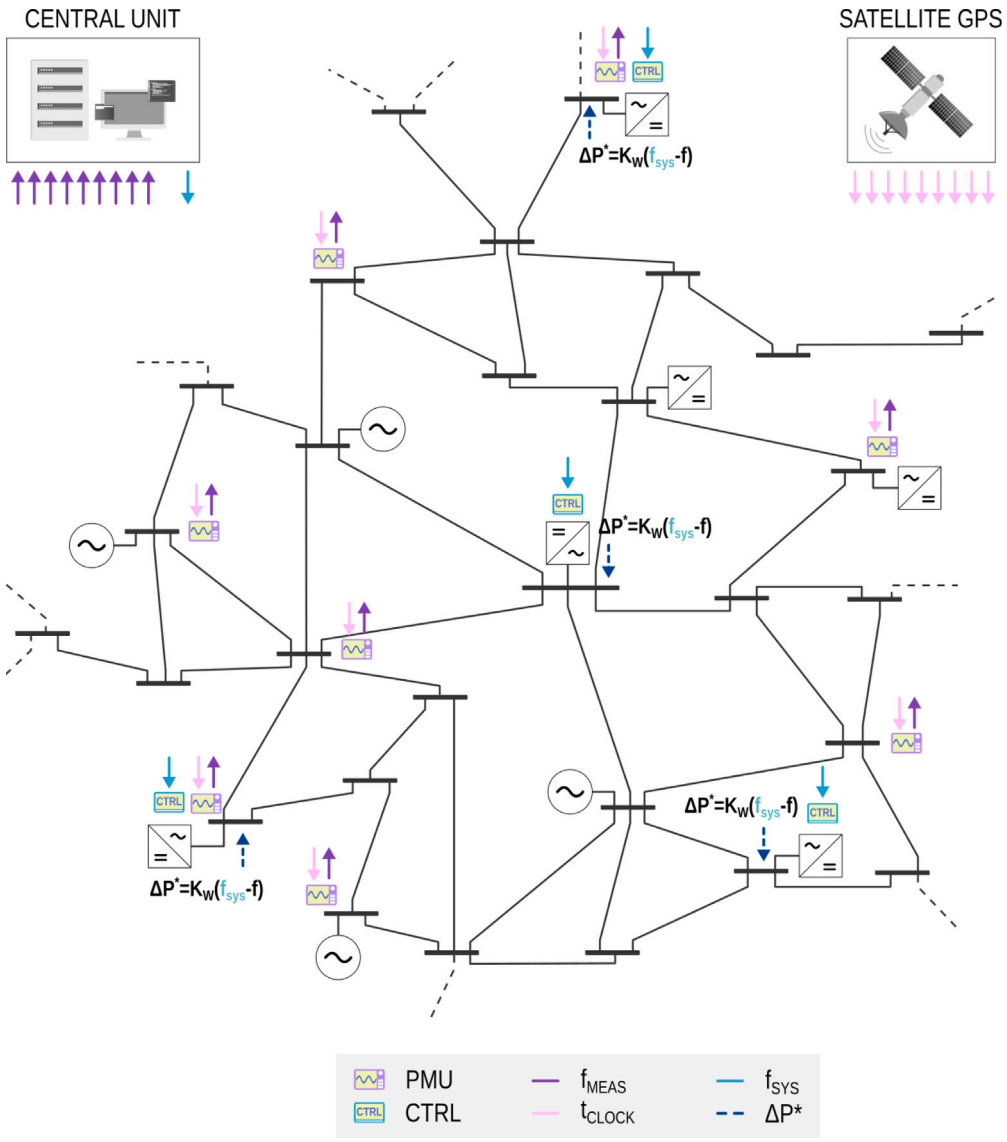

Fig. 3. Illustration of the proposed wide-synchronization control.

control structures, respectively. In the diagrams, the implementation of (1) within the active power controller of the two fundamental control strategies is delineated with shaded areas.

Although the implementation of the WSC can be achieved relying on both technologies as actuators, some fundamental differences can be pointed out. The first and main difference is that the grid-forming offers the direct availability of the terminal frequency within the active power control, whereas the grid-following requires the acquisition of the local frequency through the use of a phase-locked loop (PLL). Additionally, the grid-forming control implements by default an intrinsic power-frequency control relationship within the synchronization loop, while the grid-following control tracks the frequency changes from the grid independently of the active power control. Another important difference is that grid-forming converters are generally faster than grid-following, and the grid-forming control has the potential of providing a better damping contribution to the system. In the comparison between the two technologies, it is important to remark that the grid-following technology is a well-established standard for the control of power converters, and it is widely present in existing power systems. The grid-following technology is therefore suitable for a prompt implementation of the WSC. The grid-forming, instead, is an emerging technology, and especially in the case of interconnected power systems, there are very few grid-forming resources in operation. The grid-forming technology, however, is rapidly advancing and it is expected to play soon an essential role in the operation of the power systems. The choice of the control technology for the converters actuating the proposed WSC has therefore both advantages and disadvantages, and it might also driven by other factors depending on each specific case.

2.2. Architecture details

The architecture of the proposed WSC for a system-wise implementation is illustrated in Fig. 3.

In the proposed architecture, a central computation unit is responsible for the determination of the reference signal f_{sys}, corresponding to the average frequency of the system. For sake of illustration of the concept, the case of a single computation unit for the entire system is considered. Alternative architectures with multiple computation units for each area of the system are however possible: this decentralized control architectures will be the focus of future research, as also commented later in the article. The reference signal f_{sys} computed by the central unit is sent to the inverter-based resources involved in the control, which can be controlled either in grid-following or in grid-forming mode. The central unit computes f_{sys} processing a given number of

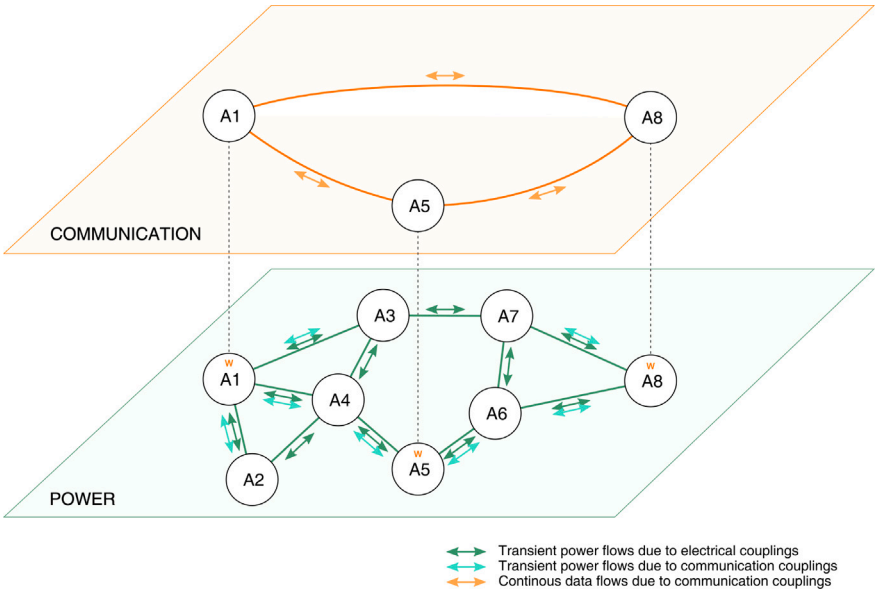

Fig. 4. Fundamental interactions in the wide-synchronization control.

frequency measurements, which are provided by the PMUs distributed in the network. The PMUs are synchronized through a GPS signal. The difference between the local frequency and the average system frequency is processed within the active power control, for a transient modification of the reference setpoint p^*, as shown in Figs. 1 and 2 with the signal Δp^*. According to the implementation, as long as there is a difference between the local frequency and the reference average frequency of the system, the control will determine a modification of the active power output of the converter. Consequently, the change in the active power will be ultimately aimed to make the local frequency of the inverter-based resource as much as possible closer to the reference signal, which represents the average of the frequencies in the different areas of the system. The implementation should also include a dead-band, to conveniently activate the control action only for values exceeding a given range of normal conditions. It is fundamental that the wide-area feedback signal f_{sys} is properly received by the resources participating in the control. In the unfortunate case of signal corrupted or not received at all, the inverter-based resource will be requested to provide a wrong amount of transient power, which may be unfeasible for the resource, with a consequent intervention of the protections. Aspects such as data integrity and cyber security are essential, and should be covered within appropriate defensive plans. It is also worth noting that the WSC will not alter the steady-state characteristics of the inverter-based resources participating in the control: the difference between the local frequency f of the inverter-based resource and the remote reference frequency f_{sys} of the control will be eventually within a range of ordinary operation, and therefore the change in the active power requested by the WSC will be annulled. At steady-state, the change in the active power given by (1) will be zero, and the inverter-based resource will provide a given active power output according to the steady-state characteristics exclusively defined by the local control scheme and settings.

Two types of areas can be then identified when representing the fundamental interactions in the proposed wide-area control: system-coupled areas and communication-coupled areas (Fig. 4). By effect of the WSC, the natural exchange of power flows across the electrical couplings of neighbouring areas for the maintaining of the synchronism will be modified. This modification is ultimately due to the transient power changes determined by the communication couplings of the areas participating in the control, and generally located far away from each other. Areas not participating in the wide-area control will also sense the transient variations in the power flows for synchronism with remote areas, and they will respond consequently. When properly implemented, this effect will then result in an effective coherency of all the areas, and thus in a significant improvement of the dynamic characteristics of the entire system. This diffusion phenomenon is conceptually depicted in Fig. 4, and it suggests the opportunity of a system-wise design of the WSC, for a full exploitation of the benefits with a minimum engagement of resources.

3. Mathematical background

The power-frequency dynamics of a generic coherent area i of the system can be described by [24]:

$$M_i\dot{\omega}_i = p_i^* - p_i - D_i\omega_i \tag{3}$$

where M_i is the inertia coefficient, equal to $2H_i$ with H_i being the total inertia constant of the area; D_i is the damping coefficient, comprehensive of the aggregated frequency droop $1/R_i$ of the area; ω_i is the per unit frequency of the area; p_i^* and p_i represent the total active power reference and active power flow of the area, respectively. The power p_i between the area i and the other areas of the system can be expressed as:

$$p_i = \sum_{j=1}^{N} K_{ij}\sin(\theta_i - \theta_j) \tag{4}$$

where N is the number of areas of the system; θ_i is the angle of the area; K_{ij} is the synchronizing coefficient between area i and area j. The angle θ_i is related to the frequency by:

$$\dot{\theta}_i = \omega_n\omega_i \tag{5}$$

where ω_i is numerically expressed with respect to the nominal angular frequency ω_n of the system. Using per unit values, the angular frequency ω and the frequency f correspond, assuming the same numeric value. When the system is linearized at a given operating point $[\omega^0\ \theta^0\ p^0]$, the coefficients K_{ij} are given by $K_{ij} = Y_{ij}V_iV_j\cos(\theta_i^0 - \theta_j^0)$, where V_i is the voltage magnitude of the equivalent node of the area i, and Y_{ij} is the equivalent admittance between area i and area j. Combining (3) and (4), for the linearized system it results:

$$M_i\dot{\omega}_i = p_i^* - \sum_{j=1}^{N} K_{ij}(\theta_i - \theta_j) - D_i\omega_i \tag{6}$$

Combining (6) and (5) and rearranging, it results:

$$M_i\ddot{\theta}_i + D_i\dot{\theta}_i + \omega_n \sum_{j=1}^{N} K_{ij}(\theta_i - \theta_j) = \omega_n p_i^* \tag{7}$$

Putting (7) in matrix form, it is possible to derive the compact notation:

$$M\ddot{\theta} + D\dot{\theta} + L\theta = p^* \tag{8}$$

where M and D are diagonal matrices of inertia and damping coefficients, and L is the admittance (or Laplacian) matrix. It is worth noting that, in the conventional case, the mutual interactions between the areas of the system are solely described by the matrix L. Eqs. (3) and (4) hold under specific assumptions, i.e. when higher-order dynamics of machines and associated controllers is neglected, lines are considered purely inductive, loads are assumed to be constant sources without dynamics, and the network is reduced to equivalent nodes, each corresponding to a coherent area. Despite the simplifying assumptions, the swing dynamics described by (3) can be conveniently used to represent the essential dynamics of the power system [25].

When the WSC is applied, (6) modifies in:

$$M_i\dot{\omega}_i = p_i^* - \sum_{j=1}^{N} K_{ij}(\theta_i - \theta_j) - D_i\omega_i + K_w(\omega_{\text{sys}} - \omega_i) \tag{9}$$

Supposing that all N areas of the system contribute to the determination of the average frequency, ω_{sys} will be given by $\omega_{\text{sys}} = 1/N \sum_{j=1}^{N} \omega_j$. Substituting ω_{sys} in (9) and rearranging, it results:

$$M_i\dot{\omega}_i = p_i^* - \underbrace{\sum_{j=1}^{N} K_{ij}(\theta_i - \theta_j)}_{\text{synchronizing coupling}} - D_i\omega_i - \underbrace{\frac{K_w}{N}\sum_{j=1}^{N}(\omega_i - \omega_j)}_{\text{damping coupling}} \tag{10}$$

In (10), two terms are pointed out. The first term corresponds to the synchronizing couplings between the areas, as well known from power systems theory and as briefly recalled before. The synchronizing couplings are enforced between system-coupled areas, through the physical interconnections of the power system. The second term is introduced by the implementation of the WSC, and it ultimately corresponds to the damping couplings between areas participating in the proposed wide-area control. The damping couplings produced by the WSC are the driving force leading to the general improvement of the dynamic characteristics of the system. The terms related to the damping coupling are enforced between communication-coupled areas, through the information carried by the signal ω_{sys} and transmitted over the communication system. The theoretical development of the damping coupling terms is illustrated with (9) and (10), and represents one of the novelty aspects of the work, providing an original mathematical formulation not present in existing literature. Referring to the matrix form in (8), it is possible to observe that, in the conventional case, $L_{ij} \neq 0$ for each i and j belonging to system-coupled areas, whereas $D_{ij} = 0$ as D is a diagonal matrix. With the application of the WSC, it results $D_{ij} \neq 0$ for each i and j belonging to communication-coupled areas. It is worth noting that, for a given area applying the WSC, the overall power flows with the neighbouring areas will be modified by effect of the proposed control, and consequently also the neighbouring areas will be driven to be closer to the average behaviour of the system, even when those areas do not participate in the control. This theoretical consideration corresponds to the diffusion phenomenon qualitatively discussed in the previous section.

The WSC is therefore aimed to introduce mutual damping couplings between the different areas of the system, contrasting the difference between the local frequencies and the average system frequency, and therefore driving the areas to be coherent with each other. Through the synchronizing couplings enforced within the power system itself, also areas not participating in the control will benefit, leading to a general improvement of the dynamic characteristics of the system.

4. Effects of latencies

4.1. Analytical discussion

The WSC has necessarily to deal with time delays and latencies, as it relies on a specific communication architecture. The expected impact of latencies is a negative destabilizing effect on the system [26]. Common countermeasures to compensate the negative effects of the latencies are model extension using Padé approximations, Smith predictor, and phase shifting with lead–lag filters [6,27,28]. Even though specific compensation techniques exist, the impact of time delays must be carefully assessed for each individual wide-area damping control scheme [7].

The effects of latencies on the proposed WSC is therefore investigated according to the following considerations. For a given area i participating in the control, the dependence on time in (1) can be made explicit, resulting in:

$$\Delta p_i^*(t) = K_w\left[f_{\text{sys}}(t - T_{di}) - f_i(t)\right] \tag{11}$$

where T_{di} is the time delay for the computation of f_{sys} and the transmission of the signal to the area i. The determination of the average frequency also modifies in:

$$f_{\text{sys}}(t) = \frac{1}{N_m}\sum_{m=1}^{N_m} f_m(t - T_{dm}) \tag{12}$$

where T_{dm} is the time delay for the acquisition of the frequency measurement m and the transmission of the signal to the central unit. From (11) and (12), it is possible to remark that the effect of latencies on the proposed wide-area damping control is a shift between actual and delayed values of f_{sys}. From (11), it can be observed that the variations of the active power $\Delta p^*(t)$ are in phase with the variations of the signal $f_{\text{sys}}(t - T_d) = f_{\text{sys}}^d$. In the ideal case of no delays, the variations of the active power Δp^* will be in phase with the actual variations of the frequency Δf_{sys}. This means that the delivered active power Δp^* will be entirely a damping power component [29,30], providing a maximum positive contribution to the damping of the system. By effect of the latencies, the variations Δf_{sys} will suffer a phase lag, and consequently the active power variations Δp^* will not be adequately in phase with the actual frequency variations Δf_{sys}, since Δp^* will have the same phase of the delayed frequency variations Δf_{sys}^d. This means that the delivered active power Δp^* will have a reduced damping power component, ultimately depending on the phase shift between actual and delayed values of the frequency f_{sys}. In the worst case, when power and frequency variations are in phase opposition, the damping contribution will be even negative, adversely amplifying the oscillations in the system and thus introducing a destabilizing effect. If the inherent damping of the system is not sufficient to counteract the destabilizing effect of the latencies, the system might be then critically unstable.

During perturbed conditions, the frequencies in the system can be affected by transient oscillations, which are typically in the range 0.1 to 2.0 Hz [29]. In the WSC, for Δf_{sys} and Δf_{sys}^d signals to be in phase opposition, the total time delay T_d should be equal to half of the period T_{osc} of the transient oscillations. Theoretically, the expected critical damping caused by the latencies is therefore periodic, and it will occur when the delays are near multiples of the half of the oscillation period. Practically, however, these transient oscillations are normally fading out within some seconds, due to the inherent damping of the system: therefore, for time delays bigger than the natural decaying time of the oscillations, the negative impact of the latencies will be significantly contained. The expected critical damping will then exhibit an attenuation as the time delays increase. In the case of no relevant transient oscillations in the frequencies during perturbed conditions, the effect of latencies will simply result in bigger instantaneous spreads between the local frequency and the delayed average frequency of the system f_{sys}^d. Consequently, the transient amount of active power

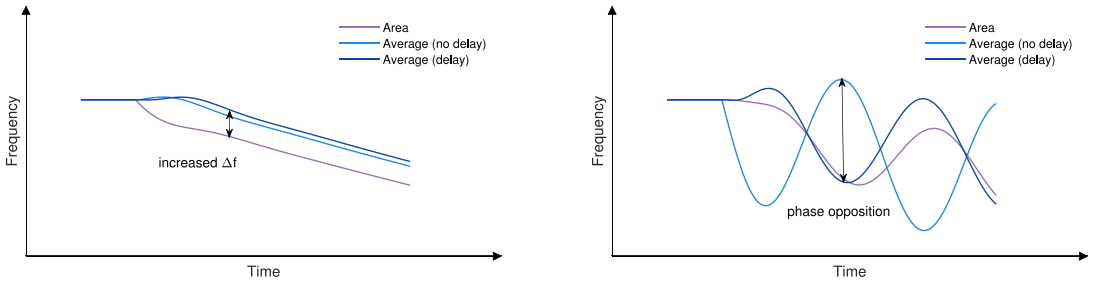

(a) No transient oscillations (b) Transient oscillations

Fig. 5. Representation of the possible effects of the latencies.

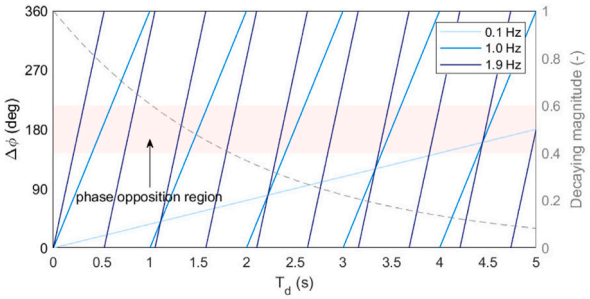

Fig. 6. Critical phase opposition region due to latencies.

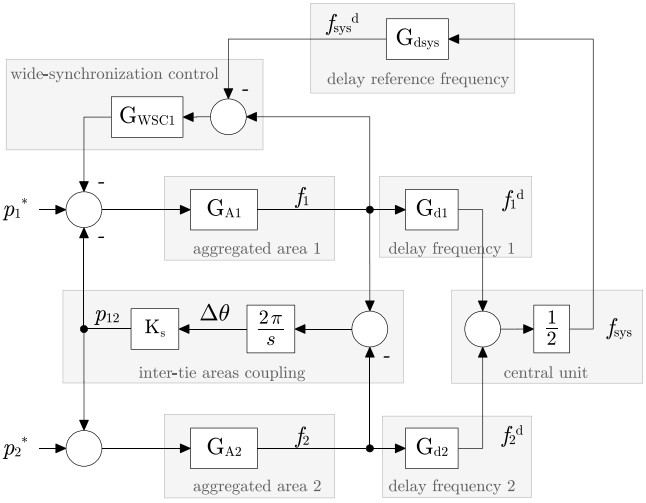

Fig. 7. Block diagram of coupled areas for latency effect investigation.

Δp^* will be larger than in the ideal case of no latencies, determining ultimately an increased inertial effect in the system.

These considerations are conceptually illustrated in Figs. 5(a) and 5(b). The figures refer to the assumption of under-frequency conditions for the system: it is worth noting that the same conclusions can be obtained assuming over-frequency conditions for the power system.

The relation between time delays and the phase opposition phenomenon is illustrated in Fig. 6. The figure shows the difference $\Delta\phi$ between the angles of actual f_{sys} and delayed f^d_{sys} signals, for three different transient oscillations frequencies. The angles are periodically wrapped between 0 and 360 degrees. The figure reports also the normalized magnitude of the oscillations for a decaying time of approximately 10 s. The critical region is identified around the value of $\Delta\phi =$ 180 degrees, where the two signals are in complete phase opposition. Considering the typical range of 0.1 to 2.0 Hz for the transient oscillations in the system, critical damping conditions due to the phase lag between actual and delayed frequency signals might occur for latencies in the range of 100 ms to few seconds. This range corresponds to the typical values of latency in wide-area applications [31,32]: a longer time has been considered in Fig. 6 only for demonstrative purposes.

For the proposed architecture, an estimation of the total latency can be done according to the following considerations. The acquisition of local frequency measurements depends on the reporting latency of the PMUs, and it can be considered in the range of 100–200 ms. The exchange of data through the communication system is strongly dependent on the chosen technology and infrastructure: for dedicated fibre-optic cables, the delay is typically around 5 μs per kilometre. The elaboration of the reference system frequency f_{sys} simply corresponds to computing the average value of the received frequencies: the CPU time required by the central unit can be estimated around 10–20 ms. The execution of the control actions in the local control system of the inverter-based resources can be assumed approximately in the range of 10–50 ms. Based on these considerations, a total round-trip latency can be approximately estimated around 200 ms. This value is consistent with the delays experienced in actual implementations of wide-area damping controls, which are found in the order of some hundreds of milliseconds [31,32].

The presented estimation of the latencies provides a constant average value T_d of the delay, which is determined according to a deterministic approach. It is important to acknowledge that delays are actually subjected to uncertainties, and in case of large interconnected systems, they will also differ from area to area. Another important observation is that the major contribution to the total time delay is due to the PMUs for the measurement of the local frequencies, as generally known for wide-area control schemes [31]. This observation suggests that, for different areas of the system, the corresponding delays for the receiving of the signal f_{sys} will be approximately of the same order, being in practice only some milliseconds apart.

4.2. Representative example

The effects of latencies on the WSC can be examined referring to the representative case of two coupled areas of the system. According to the mathematical background presented in Section 3, the dynamics of the system can be described with the block diagram of Fig. 7. In the diagram, the time delays related to the actual implementation of the control have been also considered. For sake of demonstration, the WSC is initially applied only in one area.

The transfer function $G_{\text{A}i}$ describes the aggregated dynamics of area i, and it is given by:

$$G_{\text{A}i} = K_{si}\frac{1}{M_i s + D_i} \tag{13}$$

which corresponds to (3) in the Laplace s domain, and ultimately represents the transfer function between active power and frequency. Since the mathematical system of the coupled areas is expressed in a common per unit base of $S_{\text{b}} = 100$ MVA, the factor $K_{si} = S_{\text{b}}/S_{\text{A}i}$ is

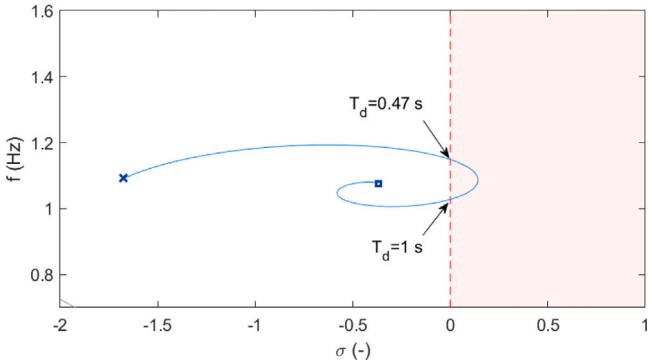

Fig. 8. Eigenvalues for time delay T_d in the range 20 ms–6 s.

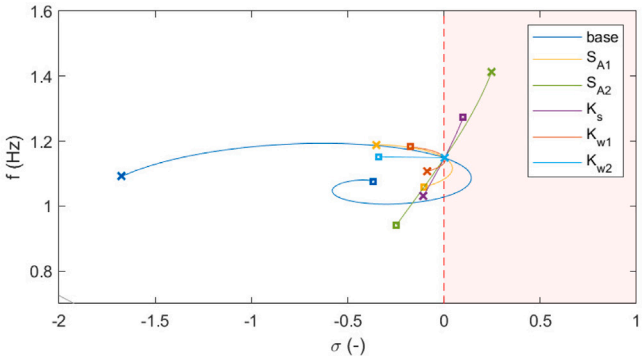

Fig. 9. Eigenvalues for different parametric ranges.

introduced for a proper base change, with S_{Ai} being the total rated power of the area i. The transfer function G_{WSCi} corresponds to (1), and it is simply given by:

$$G_{WSCi} = K_{wi} \tag{14}$$

where the gain K_{wi} takes into account the total power of the inverter-based resources participating in the control, and it is expressed in per unit of S_b. The transfer function G_d represents the modelling of the latencies in the system, and it is given by:

$$G_d = \frac{6 - 2T_d s}{6 + 4T_d s + T_d^2 s^2} \tag{15}$$

where T_d is the time delay. The modelling approach corresponds to approximating the latency with a Padé rational function. This method is commonly adopted for the representation of time delays in wide-area control schemes [33,34]. A strictly second order approximation has been here used, since rational functions with numerator and denominator of same degree introduce a jump in the output at initial conditions. The transfer function in (15) is used to represent all the latencies in the system. The blocks G_{d1} and G_{d2} represent the time delays related to the acquisition of the frequency measurements f_m and the transmission of the signals to the central unit from the PMUs of area 1 and area 2, respectively. The block G_{ds} represents the time required for the computation of f_{sys} and the transmission of the signal from the central unit to the area where the WSC is applied.

The following representative values are considered for numerical application: $S_{A1} = 1000$ MVA, $M_1 = 8$ s, $D_1 = 3.33$ pu, $K_{w1} = 50$ pu (expressed w.r.t S_{A1} base), $S_{A2} = 100$ MVA, $M_2 = 8$ s, $D_2 = 3.33$ pu, $K_s = 1.1$ pu. Using these numeric values, it is then possible to compute the oscillation modes of the coupled areas. Fig. 8 shows the eigenvalues of the system when the time delay T_d varies in the range 20 ms–6 s. The starting points are marked with crosses, whereas the ending points are marked with squares. The results confirm the theoretical considerations previously discussed. The power system with the WSC is a delay-dependent system, with multiple delay margins. The system becomes unstable for a given value of the delay, and it returns to the stable region for a successive value of the delay. It can be seen that the trajectory of the critical pair of eigenvalues is a decreasing spiral, which crosses the y-axis of the plane two times. More importantly, it can be noticed that the crossing occurs for a value of the time delay close to the half of the oscillation period. It can be easily derived that, for the considered system of coupled areas, the period T_{osc} is approximately 0.95 s: the system becomes unstable for $T_d = 0.47$ s, and then it becomes stable again for $T_d = 1$ s, approximately after half of the period T_{osc}. The critical lack of damping is then periodic, with an attenuation of the negative effect as the time delays increase. These results fully confirm the observations made in the analytical discussion.

For sake of a more comprehensive example, the computation of the oscillation modes is also repeated for different variations of the most relevant parameters of the system. The results of the sensitivity analysis are shown in Fig. 9. As before, starting points are marked with crosses, ending points with squares. In the evaluations of varying parameters, the time delay is fixed to the critical value $T_d = 0.47$ s.

The size S_{A1} of the area 1 is varied from 100 to 10,000 MVA. It can be noticed that an increase of the size of the area 1 can mitigate the critical situation caused by the latencies, eventually leading to a stable condition of the system (yellow line). It can be seen that also a reduction of S_{A1} brings the system within the stable region, since the critical lack of damping in a smaller area 1 will be more easily compensated by the other area. For varying values of the size S_{A2} of the area 2 in the range 60 to 160 MVA, it can be seen that a reduction of S_{A2} worsen the situation, whereas an increase of S_{A2} will support the stability of the system (green line), since a bigger area 2 will compensate more easily the critical lack of damping in the area 1. Varying the synchronizing coefficient K_s in the range 0.86 to 1.4 pu, it can be noticed that the strength of the interconnection between the coupled areas can also play a role: for smaller K_s and therefore for weaker inter-tie couplings, the area 2 will be marginally affected by the negative effect of the latencies in the area 1, and therefore the overall stability of the system will be improved (purple line). The gain K_{w1} of the WSC in the area 1 is varied from 10 to 1000 pu. It can be observed that, as it could have been expected, the decrease of the WSC gain K_{w1} in the area 1 determines an attenuation of the negative effect caused by the latencies, shifting the critical eigenvalue towards the left-half of the plane. It is interesting to notice that an increase of the gain K_{w1} will eventually lead the system to the stable region (orange line). This result might appear counter-intuitive, and it is explained considering that bigger values of K_{w1} will make the control action of the WSC significantly stronger. Consequently, the damping component will be intensified, and it could eventually turn to be sufficient to compensate the negative effect of the latencies. Finally, the possible participation of the area 2 in the control is also investigated, varying the gain K_{w2} from 0 to 5 pu. An interesting observation is that the additional participation of the area 2 can secure the stability of the system (light blue line), even with only a small contribution. This phenomenon can be regarded as a sort of compensation effect, and it can be clarified with the following considerations. Under the assumption of comparable dynamics in the coupled areas, it is possible to approximate the difference $\Delta\omega = \Delta\omega_1 - \Delta\omega_2$ between the frequencies of the two areas as:

$$\Delta\omega \simeq G_A \left(\Delta p + K_w \Delta\omega\right) - \underbrace{K_w \left(G_{d1} - G_{d2}\right) \omega_{sys}}_{\text{term due to latencies}} \tag{16}$$

The term due to the latencies in (16) fundamentally depends on the time delays T_{d1} and T_{d2}, which are respectively represented by the transfer functions G_{d1} and G_{d2}. These delays have generally different values: however, in practice, their values can likely be only some milliseconds apart, as detailed in the analytical discussion before. It can be then reasonably asserted $G_{d1} \simeq G_{d2}$, which means that the term due

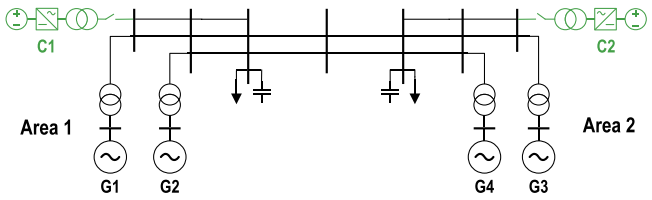

Fig. 10. Two-area four-generator benchmark system.

to latencies will be small, and the negative impact limited. This substantiates the compensation effect observed in the representative example, when both coupled areas participate in the WSC. The compensation effect will be rather effective when the coupled areas have comparable dynamics, but it will still have a certain positive effect in the general case of areas with different characteristics.

5. Case-studies

The theoretical considerations discussed in the previous sections are here demonstrated with two different case-studies, considering the standard two-area benchmark system and the large-scale model of the European power system. All simulations are based on phasor RMS models, and they are done in the commercial software Neplan with proper modifications for the implementation of the proposed WSC. The inverter-based resources have been modelled in the simulation tool as controlled sources, assuming an average model for the power converters. Grid-following converters are modelled as controlled current sources, with synchronization angle provided by the PLL. Grid-forming converters are instead modelled as controlled voltage sources, with synchronization angle provided by the power-angle control loop. In all cases, the gains K_w of the WSC are determined according to the methodology described in [17].

5.1. Two-area benchmark system

The system considered is the two-area benchmark system. The aim of this case-study is to assess the observations made in the analytical sections, and also to demonstrate the effectiveness of the WSC under critical conditions of instability. The two-area four-generator system is a well-known benchmark system: full description and data can be found in [35]. The system is shown in Fig. 10. The original model is modified for the purposes of the work, including in both areas the possibility of connecting inverter-based resources. The control system of the power converters implements either the grid-following or the grid-forming scheme: in both cases, the application of the WSC is realized with a change Δp^* in the active power output of the converter, as described in Section 2. For sake of generality, the initial steady-state operating point of the system is preserved, assuming the inverter-based resources operating with zero active and reactive power setpoints. The physical sources behind the power converters are represented as ideal DC voltage sources. The converter is represented with an average model, implementing a controlled current source in the case of grid-following, and a controlled voltage source in the case of grid-forming. Latencies are included in the model of the system according to the modelling approach described in Section 4.2. The additional data required for the simulation of the inverter-based resources are reported in Table 1.

The system is simulated for a simultaneous change in the voltage references of all generating units. This perturbation excites all the oscillation modes of the system, including inter-area and local modes. As documented in [35], the two-area system without power system stabilizers is unstable: the configuration without PSS is here assumed in the case-study, for sake of demonstration of the capabilities of the WSC. For the excitation system of the generating units, the ST1A model with transient gain reduction has been implemented. The simulations

Table 1
Parameters for IBR simulation.

Name	*Value*[a]
Converter rated power S_r	100 MVA
Active power control - Proportional gain K_{pP}	1 pu
Active power control - Integral gain K_{iP}	10 pu
Reactive power control - Proportional gain K_{pQ}	1 pu
Reactive power control - Integral gain K_{iQ}	10 pu
Phase-locked loop - Proportional gain K_{pPLL}	60 pu
Phase-locked loop - Integral gain K_{iPLL}	900 pu
AC voltage control - Proportional gain K_{pV}	1 pu
AC voltage control - Integral gain K_{iV}	100 pu
Synchronization loop - Inertia constant H	3 s
Synchronization loop - Frequency droop R	0.5 pu
Converter time constant T_c	10 ms
Filter resistance r_f	0.008 pu
Filter reactance x_f	0.1 pu
Wide-synchronization control - Proportional gain K_w	100 pu
Wide-synchronization control - Dead-band db_w	20 mHz
Wide-synchronization control - Communication delay T_d	200 ms

[a] The per unit values refer to the rated power S_r of the converter.

results are shown in Fig. 11. For different simulation cases, the figures report the frequency of one area of the system. The results of the base case show the expected instability of the system, with a progressive amplification of the oscillations (dashed lines).

From the results of Figs. 11(a) and 11(b), it can be seen that, in the ideal case of no delays, the application of the WSC effectively resolves the instability of the system, containing the oscillations and thus securing the stable operation of the system. This fundamental contribution can be provided either applying the control with grid-following or with grid-forming converters. When a time delay of $T_d = 200$ ms is considered in the simulations, it can be observed that the frequency is affected by slightly bigger oscillations, but the system has still a solid stable response. When the time delay is increased to $T_d = 900$ ms, it can be seen that there are sustained oscillations in the frequencies of the system. In this case, a difference between grid-following and grid-forming can be clearly noticed: the impact of the time delays on the control strategy when applied to grid-following converters is more critical than when applied to grid-forming converters. In particular, while the grid-forming implementation of the WSC guarantees the stability of the system even in presence of big latencies, the grid-following implementation of the WSC leads the system to the edge of the stability, as the frequency is affected by sustained oscillations with very poor damping. The difference between grid-following and grid-forming can be related to the different characteristics of the two control technologies, since the grid-following converters respond more slowly than grid-forming converters, as discussed in Section 2. Another relevant observation is that the instability due to the latencies happens for a specific value of the time delay T_d. The frequency of the critical oscillation mode is approximately 0.55 Hz, which corresponds to a period of $T_{osc} = 1.81$ s: the critical lack of damping happens for $T_d = 0.9$ s, which corresponds to half of the oscillation period T_{osc}. This result is in complete accordance with the observations made in the analytical discussion.

The results of Figs. 11(c) and 11(d) demonstrate the effectiveness of the WSC when applied within multiple areas of the system. For both grid-following and grid-forming implementation, the participation of both areas in the WSC determines an essential improvement of the dynamic characteristics of the power system. The grid-following implementation of the WSC is now stable even for the critical time delay, whereas the grid-forming implementation of the WSC is no longer affected by the sustained oscillations. These results confirm the observation made in Section 4 on the compensation effect of the latencies in case of coupled areas.

For sake of a comprehensive investigation, the modal analysis of the two-area benchmark system is also performed. The analysis is

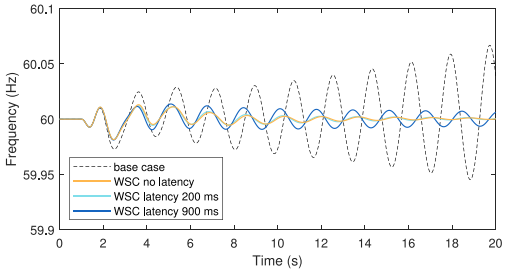

(a) WSC grid-following in area 1.

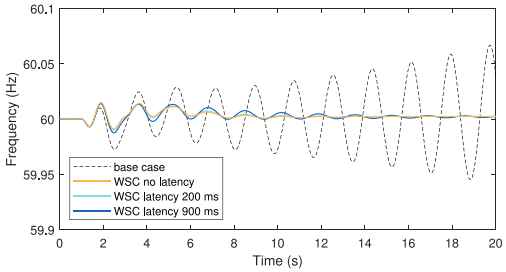

(b) WSC grid-forming in area 1.

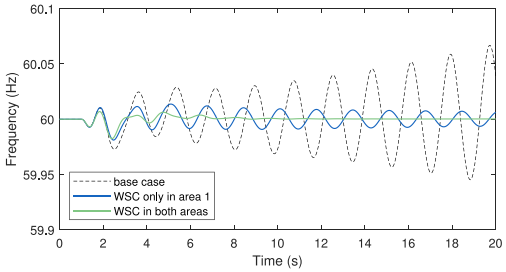

(c) WSC grid-following with $T_d = 0.9$ s.

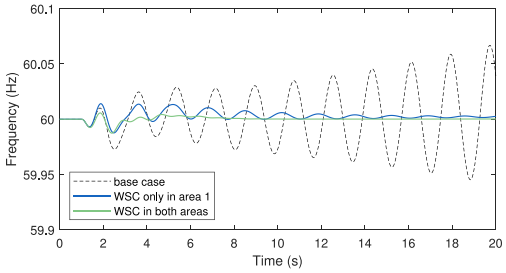

(d) WSC grid-forming with $T_d = 0.9$ s.

Fig. 11. Frequency of area 1.

computed using the small-signal stability module of Neplan. The modes of the system resulting from the calculations are shown in Fig. 12 for all the considered cases. The reach of the unstable region for a latency approximately equal to half of the oscillation period is confirmed (Fig. 12(a)). The different behaviour of grid-following and grid-forming is also demonstrated, proving the grid-forming technology to be a better option to guarantee the stability of the system even in case of critical latencies (Fig. 12(b)). Finally, the implementation of the WSC in both areas proves to bring a significant improvement to the dynamic performances of the system. The results of the modal analysis are thus in agreement with all the observations made with the time-domain simulations.

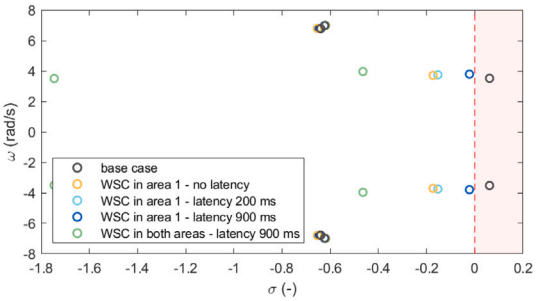

(a) WSC grid-following.

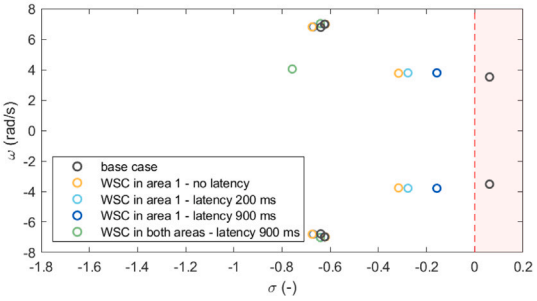

(b) WSC grid-forming.

Fig. 12. Results of modal analysis.

5.2. European power system

The system considered is the European power system. The aim of this case-study is to assess the observations made in the analytical sections, and also to prove the effectiveness of the WSC for a large power system under different inter-area oscillations. Given the extent of the Continental Europe synchronous area, this interconnected system is particularly suitable for investigating the implementation and the application of wide-area damping control schemes. The system is simulated according to the model provided by the ENTSO-E. This simulation model is a large-scale representation of the European system, it includes all zones of the different areas, and it is suitable for simulating the main frequency dynamics of the system [36–38]. To the purposes of this work, the original ENTSO-E model is modified with a specific implementation: the proposed architecture of the WSC is supplemented to the overall mathematical model, and a given amount of inverter-based resources is integrated in the system. These sources can be controlled either as grid-following or grid-forming, and they include the possibility of receiving a reference frequency signal for participation in the WSC.

In this case-study, two scenarios are examined: moderate and extensive. In the first scenario, a limited participation of inverter-based resources in the WSC is considered. The scenario designates only 5 inverter-based resources for each European country. The sources are selected among a pool of possible candidates, having rated power in the range of few hundreds of MW. This procedure leads to the values reported in Table 2 for the moderate scenario: the total power of the inverter-based resources participating in the WSC is approximately 33 GW, corresponding to the 10% of the total generated power for the considered conditions of the European system. In the second scenario, an extensive participation of inverter-based resources in the WSC is considered. The scenario selects a given number of inverter-based resources for each European country, to reach a predefined power to be committed in the WSC. The sources are selected among a pool of possible candidates, assuming a minimum rated power of some tens of MW. This procedure leads to the values reported in Table 2 for the extensive scenario: the total power of the inverter-based resources implementing the proposed wide-area damping control is approximately

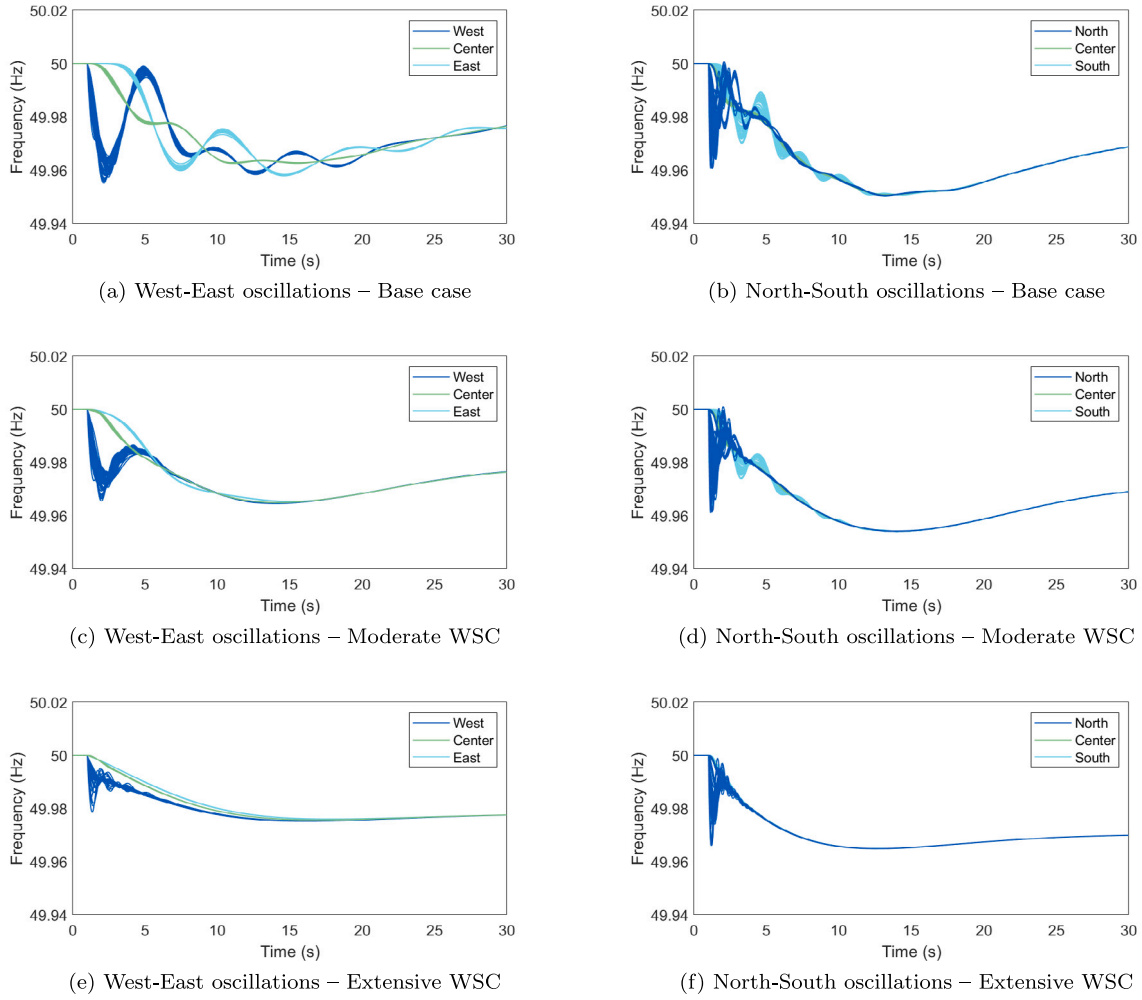

(a) West-East oscillations – Base case

(b) North-South oscillations – Base case

(c) West-East oscillations – Moderate WSC

(d) North-South oscillations – Moderate WSC

(e) West-East oscillations – Extensive WSC

(f) North-South oscillations – Extensive WSC

Fig. 13. Frequencies of selected areas in the European power system.

Table 2
Statistics of WSC participation.

Country	Moderate		Extensive	
	# IBR	Power (GW)	# IBR	Power (GW)
Germany	5	2.3	178	29.1
Spain	5	1.8	51	13.6
France	5	2.1	164	31.8
Greece	5	1.4	12	2.7
Italy	5	1.9	53	10.9
Romania	5	1.1	12	2.4
Turkey	5	1.9	74	19.2
All Europe	**100**	**33**	**710**	**153**

153 GW, corresponding to the 50% of the total generated power for the considered conditions of the European system. For both scenarios, the sources serving as actuators of the wide-area control are controlled with a mix of grid-following and grid-forming, considering the co-existence of these two technologies for a plausible integration in the power system, assuming a bigger presence of grid-following converters and a definite number of grid-forming converters. For the given number of resources participating in the control, 20% is considered to be grid-forming, and the remaining 80% is considered to be grid-following.

The inverter-based resources integrated in the model are represented as controlled sources, assuming an average model for the power converters and implementing the grid-following or grid-forming control schemes, with the application of the WSC according to the diagrams described in Section 2. Latencies are included in the model of the system according to the modelling approach described in Section 4.2. The time delays are considered varying within a given range, for a more realistic representation of the actual conditions of the system. The total round-trip delay is assumed to be variable in the range T_d = 180–300 ms. This range is determined according to the actual geographical characteristics of the European system, and it takes into account possible uncertainties in the latencies according to the considerations described in [17]. The data required for the simulation of the inverter-based resources are all as reported in Table 1, expect for the rated powers S_r, which have been properly determined for each individual inverter-based resource integrated in the system.

The system is then simulated for two power imbalances: approximately 1 GW generation loss in the western part, and approximately 1 GW generation loss in the northern part. These two disturbances are chosen as they respectively excite the main oscillation modes of the European system, the West-East mode at around 0.15 Hz, and the North-South mode at around 0.3 Hz [39]. The results of the simulations for the generation loss applied in western Europe are shown in Fig. 13(a), Figs. 13(c) and 13(e). The results of the simulations for the generation loss applied in northern Europe are shown in Fig. 13(b) Fig. 13(d), and Fig. 13(f). In all the cases, the plots display the frequencies of selected areas of the system. The countries selected for the visualization of group results are as follows. For West-East oscillations: Spain (West), Switzerland (Centre), Turkey (East). For North-South oscillations: Denmark (North), Switzerland (Centre), Italy (South). It

can be immediately observed that the proposed WSC is already effective even only with a moderate participation of inverter-based resources in the control (Figs. 13(c) and 13(d)). The damping of the system is increased, and the inter-area oscillations following the contingency are almost all eliminated. This demonstrates the diffusion phenomenon discussed in Section 2. With an extensive participation of inverter-based resources, the proposed WSC determines an exceptional improvement of the dynamics of the system (Figs. 13(e) and 13(f)). All the areas have a strongly coherent behaviour, with basically no oscillations between each other. The negative effect of the latencies has a negligible impact on the dynamics of the system, since the European synchronous area is a particularly robust system, and consequently the level of intrinsic damping is sufficient to overcome the negative effect introduced by the latencies. In this case, therefore, the latency compensation methods would not even be necessary. Additionally, the participation of all the areas of the system guarantees the positive contribution of the compensation effect discussed in Section 4. From the reported results, it is possible to observe that the application of the WSC does not alter the steady-state characteristic of the system, as the frequency reaches the same steady-state value at the end of the primary frequency control stage. It is also worth noting that the WSC can be effective against different inter-area oscillations at different oscillating frequencies, without the need of any specific tuning or particular adjustment.

6. Conclusion

The presented extension of the wide-synchronization control makes the proposed concept suitable for a general application to inverter-based resources, independently of the chosen control strategy. The active power of the resources involved in the control is transiently modified, according to the difference between the local frequency measurement and the average frequency of the system. This basic principle can be implemented either with grid-following or grid-forming converters. Both technologies can be used as actuators of the control: specific differences between the two possibilities exist, as the grid-forming offers a more flexible and effective implementation, whereas the grid-following offers a much wider readiness for actual deployment. The analytical aspects presented in the mathematical discussion indicate that the implementation of the WSC ultimately corresponds to the introduction of damping couplings between the areas participating in the control. By effect of the WSC, the differences between the local frequencies of all the areas and the average frequency of the system will be significantly reduced or even eliminated, leading to a general improvement of the dynamic characteristics of the entire system. The examination of the impact of the latencies on the proposed control shows that, by effect of the time delays, the variations of the active power might not be adequately in phase with the actual frequency variations, with a consequent reduction of the damping power contribution. Critical conditions can occur only if the inherent damping of the system is not sufficient to counteract the destabilizing effect of the time delays. The analysis also shows that the proposed WSC has some resilience against the negative effect of the latencies. The application of the WSC to two different case-studies confirms the observations made in the analytical sections. Both case-studies prove how the application of the proposed wide-area control can lead to a relevant improvement in the dynamic characteristics of the system. The first case-study demonstrates the capability of the control to secure the stability of the system even under critical conditions, showing the results also in terms of small-signal stability analysis. The second case-study indicates that the proposed control performs markedly well in large interconnected systems, increasing the system damping for different transient phenomena and inter-area oscillating frequencies, even without any particular adjustment.

The wide-area damping control presented in this work is particularly addressed to TSOs, as it has the potential to significantly improve the dynamic characteristics of the system. However, also inverter manufacturers and power plant owners can be related. The proposed WSC has several open points, which can be addressed in further research and developments of the concept. Number and localization of the required measurements is certainly an aspect which can be investigated, with rigorous and detailed methodologies. The eligibility of the inverter-based resources to be operated as actuators in the WSC is another aspect worth investigating. The opportunity of alternative architectures based on multiple computation units might be also explored with further studies. An important aspect is the possibility of a decentralized control, where the single control units in each area of the system should coordinate and interact with each other to achieve the required performances. Finally, from the point of view of a practical deployment of the proposed control architecture, it is fundamental to consider aspects such as data integrity and cyber security, robustness against communication failures, resilience under severe system split contingencies.

CRediT authorship contribution statement

Mariano G. Ippolito: Writing – review & editing, Supervision. **Rossano Musca:** Writing – original draft, Software, Methodology, Formal analysis, Data curation, Conceptualization.

Declaration of competing interest

The authors declare that they have no known competing financial interests or personal relationships that could have appeared to influence the work reported in this paper.

Data availability

The data that has been used is confidential.

References

[1] Rafique Z, Khalid HM, Muyeen S, Kamwa I. Bibliographic review on power system oscillations damping: An era of conventional grids and renewable energy integration. Int J Electr Power Energy Syst 2022;136:107556. http://dx.doi.org/10.1016/j.ijepes.2021.107556.

[2] Zacharia L, Asprou M, Kyriakides E, Polycarpou M. Effect of dynamic load models on WAC operation and demand-side control under real-time conditions. Int J Electr Power Energy Syst 2021;126:106589. http://dx.doi.org/10.1016/j.ijepes.2020.106589.

[3] Zenelis I, Wang X. A model-free sparse wide-area damping controller for inter-area oscillations. Int J Electr Power Energy Syst 2022;136:107609. http://dx.doi.org/10.1016/j.ijepes.2021.107609.

[4] Chen X, Jiang Y, Terzija V, Lu C. Review on measurement-based frequency dynamics monitoring and analyzing in renewable energy dominated power systems. Int J Electr Power Energy Syst 2024;155:109520. http://dx.doi.org/10.1016/j.ijepes.2023.109520.

[5] Azizi S, Rezaei Jegarluei M, Sánchez Cortés J, Terzija V. State of the art, challenges and prospects of wide-area event identification on transmission systems. Int J Electr Power Energy Syst 2023;148:108937. http://dx.doi.org/10.1016/j.ijepes.2022.108937.

[6] Mira-Gebauer N, Rahmann C, Álvarez Malebrán R, Vittal V. Review of wide-area controllers for supporting power system stability. IEEE Access 2023;11:8073–95. http://dx.doi.org/10.1109/ACCESS.2023.3237576.

[7] Zhang X, Lu C, Liu S, Wang X. A review on wide-area damping control to restrain inter-area low frequency oscillation for large-scale power systems with increasing renewable generation. Renew Sustain Energy Rev 2016;57:45–58. http://dx.doi.org/10.1016/j.rser.2015.12.167.

[8] Younis MR, Iravani R. Wide-area damping control for inter-area oscillations: A comprehensive review. In: Proceedings of the 2013 IEEE electrical power & energy conference. 2013.

[9] Wide area monitoring protection and control systems – Decision support for system operators. Tech. rep., CIGRE Technical Brochures, C2 Power system operation and control Committee; 2023.

[10] Radwan MM, Azmy AM, Ali GE, ELGebaly AE. Optimal design and control loop selection for a STATCOM wide-area damping controller considering communication time delays. Int J Electr Power Energy Syst 2023;149:109056. http://dx.doi.org/10.1016/j.ijepes.2023.109056.

[11] Kumar A, Bhadu M. Wide-area damping control system for large wind generation with multiple operational uncertainty. Electr Power Syst Res 2022;213:108755. http://dx.doi.org/10.1016/j.epsr.2022.108755.
[12] Darabian M, Bagheri A. Design of adaptive wide-area damping controller based on delay scheduling for improving small-signal oscillations. Int J Electr Power Energy Syst 2021;133:107224. http://dx.doi.org/10.1016/j.ijepes.2021.107224.
[13] Ranjbar S, Al-Sumaiti AS, Sangrody R, Byon Y-J, Marzband M. Dynamic clustering-based model reduction scheme for damping control of large power systems using series compensators from wide area signals. Int J Electr Power Energy Syst 2021;131:107082. http://dx.doi.org/10.1016/j.ijepes.2021.107082.
[14] Noori A, Jafari Shahbazadeh M, Eslami M. Designing of wide-area damping controller for stability improvement in a large-scale power system in presence of wind farms and SMES compensator. Int J Electr Power Energy Syst 2020;119:105936. http://dx.doi.org/10.1016/j.ijepes.2020.105936.
[15] Yao W, Jiang L, Wen J, Wu Q, Cheng S. Wide-area damping controller of FACTS devices for inter-area oscillations considering communication time delays. IEEE Trans Power Syst 2014;29(1):318–29. http://dx.doi.org/10.1109/TPWRS.2013.2280216.
[16] Itiki R, Libonati F, Burgués H, Martini M, Essakiappan S, Manjrekar M, et al. A proposed wide-area stabilization system through a large-scale fleet of electric vehicles for grid. Int J Electr Power Energy Syst 2022;141:108164. http://dx.doi.org/10.1016/j.ijepes.2022.108164.
[17] Musca R, Riva Sanseverino E, Zizzo G, Giannuzzi G, Pisani C. Wide-Synchronization Control for Power Systems with Grid-Forming Converters. IEEE Trans Power Syst 2023. http://dx.doi.org/10.1109/TPWRS.2023.3334876, (Early Access).
[18] Musca R, Just H. Damping-enhanced schemes and wide-synchronization control for grid-forming converters. In: IET conference proceedings, 22nd wind & solar integration workshop. 2023.
[19] Musca R, Riva Sanseverino E, Zizzo G, Giannuzzi G, Pisani C. The opportunity of grid-forming converters in the wide-area control of power systems. In: IET conference proceedings, 21st wind & solar integration workshop. 2022, http://dx.doi.org/10.1049/icp.2022.2736.
[20] Li Y, Gu Y, Green TC. Revisiting grid-forming and grid-following inverters: A duality theory. IEEE Trans Power Syst 2022;37(6):4541–54. http://dx.doi.org/10.1109/TPWRS.2022.3151851.
[21] Musca R, Gonzalez-Longatt F, Gallego Sánchez CA. Power system oscillations with different prevalence of grid-following and grid-forming converters. Energies 2022;15(12). http://dx.doi.org/10.3390/en15124273, (4273).
[22] Ippolito MG, Musca R, Riva Sanseverino E, Zizzo G. Frequency dynamics in fully non-synchronous electrical grids: A case study of an existing island. Energies 2022;15(6). http://dx.doi.org/10.3390/en15062220.
[23] Ippolito MG, Musca R, Zizzo G. Generalized power-angle control for grid-forming converters: A structural analysis. Sustain Energy Grids Netw 2022;31(100696). http://dx.doi.org/10.1016/j.segan.2022.100696.
[24] Dörfler F, Bullo F. Synchronization in complex networks of phase oscillators: A survey. Automatica 2014;50(6):1539–64.
[25] Dörfler F, Jovanović MR, Chertkov M, Bullo F. Sparse and optimal wide-area damping control in power networks. In: 2013 American control conference. 2013, p. 4289–94. http://dx.doi.org/10.1109/ACC.2013.6580499.
[26] Ömer Aydın, Sönmez Şahin, Ayasun S. Determination of stability delay margins for multi-area load frequency control systems with incommensurate time delays through eigenvalue tracing method. Int J Electr Power Energy Syst 2022;137:107821. http://dx.doi.org/10.1016/j.ijepes.2021.107821.
[27] Liu Z, Song B, Sun Y, Yang Y. Time-varying delays and their compensation in wide-area power system stabilizer application. Int J Electr Power Energy Syst 2015;73:149–56. http://dx.doi.org/10.1016/j.ijepes.2015.04.005.
[28] Darabian M, Bagheri A. Design of adaptive wide-area damping controller based on delay scheduling for improving small-signal oscillations. Int J Electr Power Energy Syst 2021;133:107224. http://dx.doi.org/10.1016/j.ijepes.2021.107224.
[29] Kundur P, Balu NJ, Lauby MG. Power system stability and control. New York, USA: McGraw-Hill; 1994.
[30] Schäfer B, Matthiae M, Timme M, Witthaut D. Decentral Smart Grid Control. New J Phys 2015;17(015002). http://dx.doi.org/10.1088/1367-2630/17/1/015002.
[31] Peng L, Xiaochen W, Chao L, Jinghai S, Jiong H, Jingbo H, et al. Implementation of csg's wide-area damping control system: Overview and experience. In: Proceedings of the 2009 IEEE/PES power systems conference and exposition. 2009.
[32] La Scala M, De Benedictis M, Bruno S, Grobovoy A, Bondareva N, Borodina N, et al. Development of applications in WAMS and WACS: An international cooperation experience. In: Proceedings of the 2006 IEEE power engineering society general meeting. 2006.
[33] Zhang S, Vittal V. Design of wide-area power system damping controllers resilient to communication failures. IEEE Trans Power Syst 2013;28(4):4292–300. http://dx.doi.org/10.1109/TPWRS.2013.2261828.
[34] Dotta D, e Silva AS, Decker IC. Wide-area measurements-based two-level control design considering signal transmission delay. IEEE Trans Power Syst 2009;24(1):208–16. http://dx.doi.org/10.1109/TPWRS.2008.2004733.
[35] Benchmark systems for small-signal stability analysis and control. Tech. rep., IEEE Power and Energy Society, IEEE Power System Dynamic Performance Committee; 2015.
[36] ENTSO-E. Initial dynamic model of continental europe. 2022, https://www.entsoe.eu/publications/system-operations-reports/#entso-e-dynamic-model-of-continental-europe. (Last accessed on 2022).
[37] Semerow A, Höhn S, Luther M, Sattinger W, Abildgaard H, Garcia AD, et al. Dynamic study model for the interconnected power system of continental europe in different simulation tools. In: Proceedings of the 2015 IEEE Eindhoven PowerTech. 2015.
[38] Busarello L, Musca R. Impact of high share of converter-interfaced generation on electromechanical oscillations in Continental Europe power system. IET Renew Power Gener 2020;14(19):3918–26. http://dx.doi.org/10.1049/iet-rpg.2020.0489.
[39] Grebe E, Kabouris J, Barba SL, Sattinger W, Winter W. Low frequency oscillations in the interconnected system of continental europe. In: Proceedings of the *IEEE PES general meeting*. 2010.